In Situ Lateral Stress Measurement in Glaciolacustrine Seattle Clay Using the Pressuremeter

Oliver Hoopes, A.M.ASCE[1]; and John Hughes, M.ASCE[2]

Abstract: Pressuremeter testing was conducted for the State Route (SR) 99 Bored Tunnel project in Seattle, Washington, to estimate in situ soil stress-deformation parameters along the tunnel alignment. Many of the tests were conducted in a very stiff to hard glaciolacustrine clay known as Seattle clay. This unit is historically known for deep-seated slope failures and many of these failures have been attributed to the release of high, locked-in lateral stresses. Estimation in situ lateral stresses along the tunnel alignment was a primary focus of the exploration program. Due to the hard consistency of this unit and the potential for cobbles, neither self-boring pressuremeter nor dilatometer testing was feasible; therefore, prebored pressuremeter testing was used. Using several lateral stress estimation techniques, including a novel in situ creep testing approach, the in situ lateral stresses in the Seattle clay were estimated to be significantly higher than what would be expected by assuming a simple, laterally constrained, vertical loading and unloading stress path due to glaciation. Deformational features commonly encountered in Seattle clay indicate its stress history also has included significant lateral shearing. The memory of this shearing within the fabric of the clay may influence the in situ stress state and response to lateral unloading. **DOI: 10.1061/(ASCE)GT.1943-5606.0001077.**

Author keywords: In situ lateral stress; Geostatic stress; Stiff clay; Glacial deformation; Pressuremeter; Creep testing; Glaciolacustrine clay; Fissured clay.

Introduction

An extensive geotechnical exploration program was conducted along the alignment of the proposed State Route (SR) 99 Tunnel Project. The roughly 2.6-km-long bored tunnel is designed to run north-south below downtown Seattle (Fig. 1) at depths ranging from approximately 30 to 85 m below the ground surface. At 17.7 m in diameter, the SR-99 tunnel would be the largest bored tunnel in soil in the world.

The SR-99 tunnel exploration program included over 120 pressuremeter tests (PMT), which were used to estimate in situ soil stress-deformation parameters along the tunnel alignment. Many of the tests were conducted in a very stiff to hard glaciolacustrine clay known as Seattle clay. This unit is historically known for deep-seated slope failures and many of these failures have been attributed to the release of high, locked-in lateral stresses. In the early stage of the PMT program, there were indications of a high in situ lateral stress from a visual inspection of the pressuremeter data. During the final 10 PMTs in this clay, the lateral stresses were considered in more detail; this is the focus of this paper.

In situ lateral stresses, σ_{h0}, were a primary focus of the pressuremeter testing program as they impact the earth pressure balance machine face pressure design, tunnel liner design, and are used in finite-element modeling for settlement estimation. Owing to the hard consistency of this unit and the potential for cobbles, neither self-boring pressuremeter nor dilatometer testing was feasible and, therefore, prebored pressuremeter testing was used. Because most published procedures for estimating σ_{h0} involve examination of the initial portion of the pressuremeter stress-strain curve and because this portion of the curve is the most impacted by preboring-related disturbance (Marsland and Randolph 1977), estimation of in situ σ_{h0} in Seattle clay was particularly challenging.

In this study, σ_{h0} was primarily estimated using constitutive model, curve-fitting techniques using pressuremeter data and using a heretofore unpublished, experimental method that relies on iterative creep testing. These methods both make use of the postyield and unloading portions of the pressuremeter stress-strain curves. Due to the higher stresses at these latter test stages, the annular zone of stressed soil is larger than at the beginning of the test and, therefore, a larger percentage of the soil response is thought to be derived from the intact soil beyond the annulus of soil most disturbed by the preboring process. As such, it is reasoned that these methods are less impacted by borehole disturbance than other methods that rely on the initial stages of the tests.

The pressuremeter-derived in situ lateral stresses presented here were compared to results of previous studies in Seattle clay and to stresses estimated using relationships between the overconsolidation ratio (OCR = effective vertical yield stress, σ'_{vY}, divided by the current effective vertical stress, σ'_{v0}) and the coefficient of lateral earth pressure at rest (K_0 = effective in situ lateral stress, σ'_{h0}, divided by σ'_{v0}), which assumes the clay has undergone one-dimensional, laterally constrained loading and unloading (hereafter referred to as simple loading and unloading). The in situ lateral stresses in the Seattle clay were estimated to be significantly higher than what would be expected by assuming a simple loading and unloading stress path due to glaciations and rebound. Deformational features commonly encountered in Seattle clay indicate its stress history also has included significant lateral shearing. The memory of this shearing within the fabric of the clay may influence the in situ stress state and response to lateral unloading.

Downtown Seattle Soil and Seattle Clay

The geology along the bored tunnel portion of the SR-99 tunnel alignment is quite diverse (Fig. 1) and primarily consists of soil that

[1]Senior Engineer, Shannon and Wilson, Inc., 400 N. 34th St., Suite 100, Seattle, WA 98103 (corresponding author). E-mail: ohoopes@gmail.com

[2]President, Hughes Insitu Engineering, Ltd., 3009 St. Andrews Ave., Vancouver, BC, V7N 1Z5 Canada.

Note. This manuscript was submitted on August 13, 2012; approved on November 23, 2013; published online on December 24, 2013. Discussion period open until May 24, 2014; separate discussions must be submitted for individual papers. This paper is part of the ***Journal of Geotechnical and Geoenvironmental Engineering***, © ASCE, ISSN 1090-0241/04013054 (11)/$25.00.

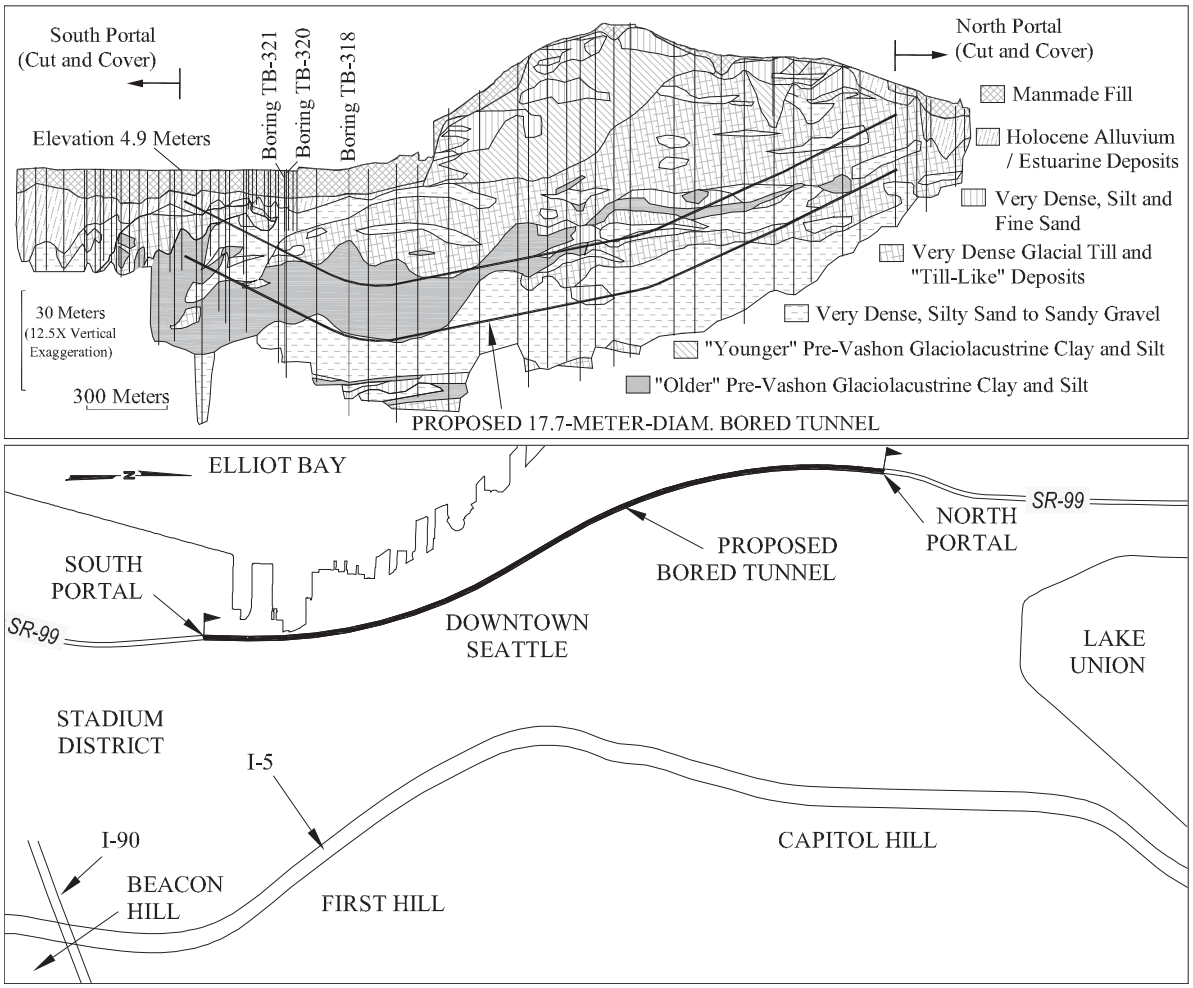

Fig. 1. Tunnel alignment plan and simplified geologic profile

has been subjected to a complex stress history that includes at least six glaciations (Troost and Booth 2008; Thorson 1989). During the most recent glaciation, identified locally as the Vashon stade of the Fraser glaciation (approximately 14,000 to 17,000 years before present at Seattle), the Puget lobe of the Cordilleran ice sheet is estimated to have been about 900-m thick in the Seattle area (Thorson 1989). Proglacial outwash sediments, named the Great Lowland Fill (GLF), were deposited ahead of the Puget lobe during the Vashon glaciation up to an about level surface elevation of 140 m in the Seattle area. This unit is still present in many hills in the Puget Sound area (identified locally as Esperance Sand or Vashon Advance Outwash), but the majority of the original GLF was eroded by high-pressure, subglacial meltwater (Booth 1994; Booth and Hallet 1993).

Booth (1991) estimated subglacial meltwater pressures to be roughly equal to the total overburden ice pressure beneath the majority of the ice lobe, resulting in low *net* effective normal stress increase under the majority of the ice sheet during the glacial occupation (Booth 1991). However, as indicated in Fig. 2, Booth (1991) estimated the average net effective normal stress increase from the ice overburden at the southern margin of the ice lobe to have been on the order of about 1 MPa, and noted that this stress could be raised locally by up to a factor of three because of episodic, seasonal drainage events. The maximum past vertical effective stress (σ'_{vY}) of the deep glaciolacustrine clay along the tunnel alignment, estimated using one-dimensional consolidation test data later in this paper, was likely caused in part by this net ice stress but primarily from the

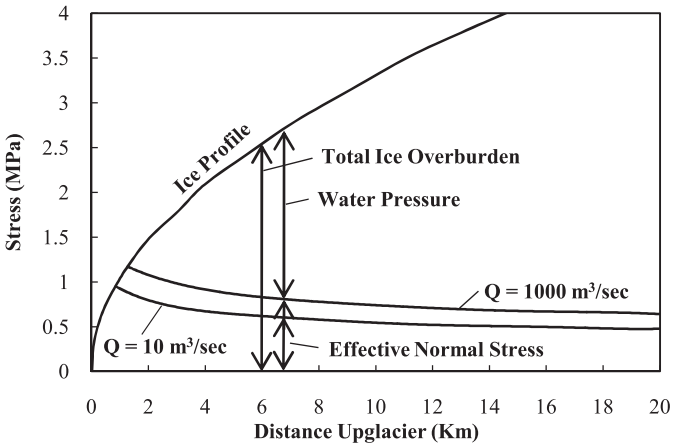

Fig. 2. Estimated total and effective normal stresses beneath the Puget Lobe of the Cordilleran Ice Sheet for different subglacial meltwater discharge rates, Q (adapted from Booth 1991)

roughly 140-m-thick GLF soil surcharge. These two loads likely would have been applied concurrently to the deep clay during the recession of the Vashon glaciation.

The soil of primary interest in this paper is a pre-Vashon-age (Quaternary), glaciolacustrine clay (Qpgl). This unit is very similar to

the younger and better known Vashon-age glaciolacustrine Lawton clay (Qvgl), except it has been subjected to more than one glaciation. Qpgl can be distinguished from Lawton clay if it is stratigraphically below a group of paleosols known as the Olympia beds. In this paper, the term Seattle clay is used to refer all glaciolacustrine clay in the greater Seattle area. These deposits are the result of the deposition of suspended sediments in proglacial lakes in the Puget Sound Lowland and, in the case of clay along the tunnel alignment, have been loaded by the ice of at least two glacial advances and the GLF during the Vashon stade. Seattle clay deposits generally consist of very stiff to hard, silty clay and clayey silt rock flour with scattered beds and partings of silt and silty, fine sand. These deposits include both low- and high-plasticity clay and range from laminated to massive. As indicated in Fig. 1, the Qpgl typically is capped by a layer of very dense glacial till (Qpgt) throughout the tunnel alignment and commonly is underlain by dense to very dense sand and gravel glacial outwash deposits.

Index and strength parameters from a database that includes tests from SR-99 Tunnel and Beacon Hill Light Rail Tunnel projects are summarized in Tables 1 and 2. Descriptive soil parameters and estimated in situ stresses for the 10 balance pressure creep tests used in this study are presented in Table 3.

Typical of many heavily overconsolidated clays throughout the world, these deposits commonly contain scattered slickensides and hairline fissures. Many researchers have concluded these are the result of the application (compression) and withdrawal (rebound) of the immense glacial-related loads described previously (Palladino and Peck 1972; Strazer et al. 1972; Squier and Klasell 1989; Miller 1989; Converse Consultants, "Report on Geotechnical Investigation, Proposed I-90 East Limits of Mercer Island Tunnel to South Bellevue Interchange," unpublished report). However, many Qpgl and some Qvgl deposits have been documented to contain zones of intensely sheared (low angle), blocky, and slickensided highly variable vertical and horizontal dimensions (from a few feet to tens of feet). These deformed zones have been encountered near the ground surface as well as at depths greater than 43 m in some of the SR-99 tunnel borings. A typical example of this deformation from a site about 11 km to the northeast of the tunnel site is depicted in Fig. 3.

Based on the SR-99 tunnel explorations and other large infrastructure projects in the greater Seattle area including the Beacon and First Hill Light Rail Tunnels, the SR-520 Floating Bridge Replacement project, Seattle Monorail project (not constructed), and many other smaller projects in the area, these deformation zones appear to be widespread within the Qpgl geologic unit as a whole. The intensity of the deformation in these zones (Fig. 3) appears to be too great to be caused by one-dimensional unloading alone. However, the spatial variability and the apparently discontinuous nature of the deformation zones do not support a sole hypothesis of ancient landsliding. Some geologists have theorized that some of these deformation zones may be related to the Seattle Fault (Troost and Booth 2008). While this may be true in some of those cases within the Seattle Fault Zone, many of the projects previously listed are located several miles north of mapped splays of the Seattle Fault Zone. Another explanation may be that the deformation zones were caused by passive shearing (glacial bulldozing) owing to the advancing ice lobe and formation of the overlying glacial till. It is possible the glacial ice caused fronts of deep passive shear stresses below the southern ice lobe boundary to sweep through the underlying clay as the ice invaded southward. The combination of high subglacial water pressure gradients (Fig. 2), highly variable geologic layering (Fig. 1), and uneven ground surface topography may have led to localized rather than homogeneous or widespread passive failures within the clay and silt units.

Fig. 4 presents a conceptualization of the stress history of a theoretical sample of Qpgl at a depth of about 29 m in the vicinity of borings TB-318, TB-320, and TB-321 (Fig. 1). Details of Fig. 4 are revisited subsequently, but a brief summary is as follows:

Table 1. Qpgl Index Parameters from SR-99 Tunnel and Beacon Hill Light Rail Projects

Parameter (%)	Mean	SD	Data points
LL	56	15	868
PI	31	16	868

Table 2. Qpgl Strength Parameters from Beacon Hill Light Rail Project

Specimen fabric	Data points	ϕ'^{a} (degree)	c'^{a} (kPa)
Relatively intact	63	29	57
Discontinuous slickensides	10	22	26
Slickensided	6	16	0

[a]Mohr-Coulomb strength parameters derived from isotropically consolidated undrained triaxial compression tests.

Table 3. Balance Pressure PMT Summary

							Estimated K_0 range by method				
Test number	Boring	Depth (m)	PI[a] (%)	σ'_{v0} (kPa)	Estimated OCR range	Clay fabric[a]	Mayne and Kulhawy (1982)	Brooker and Ireland (1965)	PMT model analysis	PMT BPC	Number of BPC trial pressures
119	TB-318	28.6	36	287	5–15	deformed	1.1–1.9	1.2–1.7	1.5	1.7–2.1	2
118	TB-318	29.0	36	291	5–15	deformed	1.1–1.9	1.2–1.7	2.8	2.8–2.9	3
129	TB-318	37.7	27	401	4–11	intact	1–1.6	1–1.7	1.9	2.0–2.2	3
128	TB-318	38.2	27	406	4–11	intact	1–1.6	1–1.7	2.2	2.3–2.6	3
130	TB-318	41.2	51	442	4–10	intact	1–1.6	1.3–1.5	1.8	1.8–1.9	3
137	TB-321	43.5	32	422	4–10	intact	1–1.6	1–1.6	1.2	1.2	5
136	TB-321	44.0	32	427	4–10	intact	1–1.6	1–1.6	1.3	1.1	5
132	TB-320	44.3	50	473	4–9	deformed	1–1.5	1.3–1.5	1.8	1.8–1.9	3
139	TB-321	46.9	42	453	4–10	intact	1–1.6	1.2–1.6	0.9	0.8–0.9	3
138	TB-321	47.3	42	457	4–10	intact	1–1.6	1.2–1.6	0.9	0.9	3

Note: BPC = balance pressure creep.

[a]Based on soil samples immediately above and/or below PMT.

J. Geotech. Geoenviron. Eng. 2014.140.

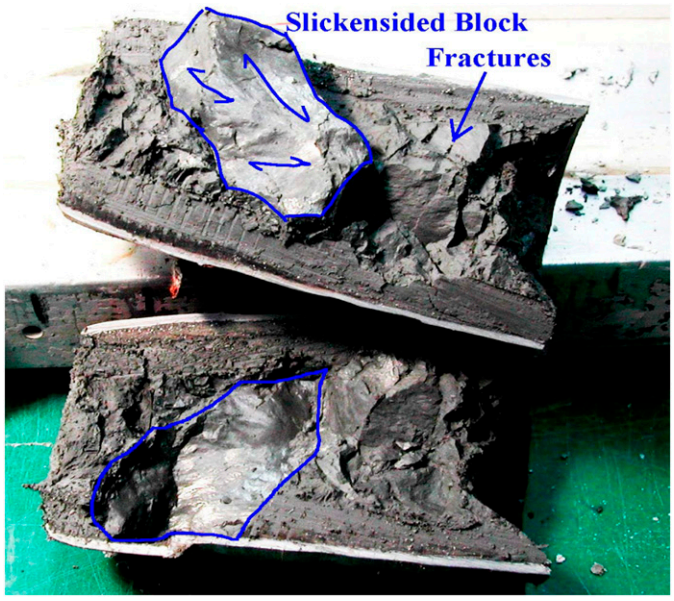

Fig. 3. Highly deformed specimen of Qpgl retrieved from a boring near SR-520 and Bellevue Way at a depth of 6.4 m; tube sampler is 7.6 cm diameter (courtesy of Shannon & Wilson, Inc., with permission)

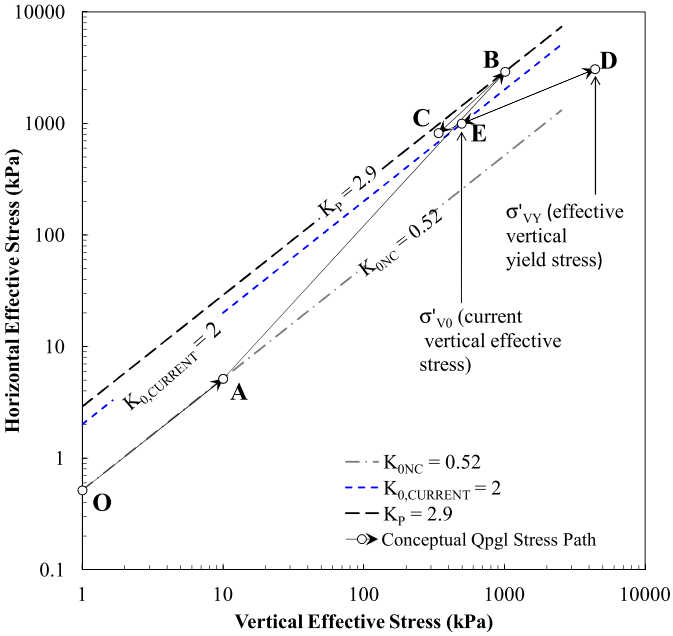

Fig. 4. Conceptualization of Qpgl stress history (assumes two glaciations)

O to A: Deposition in proglacial lake during pre-Vashon glaciation (Qpgl) occurred.
A to B: Pre-Vashon Puget Lobe advance caused subglacial passive shearing and formation of overlying Qpgt. Point B assumes 1 MPa net effective vertical stress increase (from Fig. 2).
B to C: Simple unloading from pre-Vashon glaciation. Assumed ground surface at current upper pre-Vashon soil contact (possible erosion not accounted for).
C to D: Deposition in Vashon-age proglacial lake such that Qvgl was deposited and subsequently covered by the GLF and then further overridden by the Puget Lobe of the Vashon glaciation (assumed simple loading only occurred; that is, Qpgl does not feel passive shear stress increase during to advancement of Vashon Puget lobe due to cushion of up to 140-m thick GLF deposit between ice and clay).
D to E: Simple unloading occurred because of GLF erosion and Vashon Puget lobe retreat.

For simplicity, only one pre-Vashon glaciation (i.e., two glaciations are shown including one pre-Vashon glaciation from O to B and the Vashon glaciation from C to D) is assumed in Fig. 4. The Qpgl in the current study has been subjected to at least two and perhaps as many as five pre-Vashon glaciations. Because the in situ horizontal effective stress cannot exceed the passive stress state, the K_P line in Fig. 4 would have imposed an upper boundary causing the stress path between additional pre-Vashon glacial loadings to likely cycle between stress states similar to B, C, D, and E rather than ratcheting upward with each glaciation.

Local experience has shown that slope failures are common in cuts in Seattle clay. Large-strain, ring-shear testing and back analyses of landslides in Seattle clay typically have resulted in residual effective stress friction angles of 13–18° [Palladino and Peck 1972; Andrews et al. 1966; Johnson 1989; Converse Consultants, "Report on Geotechnical Investigation, Proposed I-90 East Limits of Mercer Island Tunnel to South Bellevue Interchange," unpublished report; Miller 1989; Washington State DOT (WSDOT) 2012]. A review of several large infrastructure project geotechnical studies [Link Light Rail Tunnels, Interstate 5 Freeway construction, I-90 Mercer Island, and several downtown high-rise structures as described by Laprade (1982)] reveals that high in situ locked-in lateral stresses are typical in the unit (Palladino and Peck 1972; Strazer et al. 1972; Sherif and Wu 1971; Sherif and Strazer 1973; WSDOT 2012). As postulated by Skempton et al. (1969) and Rowe (1972), high in situ lateral pressures would tend to keep joints and fissures closed within the mass but these discontinuities would begin to open up upon lateral stress relief (e.g., by cutting into a slope). Coupled with periods of heavy, sustained rainfall events and the well-established trend that porewater pressures in very stiff clays are initially negative upon application of shear stresses (i.e., they tend to dilate), the opening of discontinuities in these soils can allow water infiltration and cause the in situ strength to degrade from very high undrained strengths to fully softened and eventually residual strength. As shown by Duncan and Dunlop (1969), high K_0 conditions cause maximum in situ shear stresses to be significantly higher in soil cuts. This can greatly reduce the available shear strength and lead to progressive failure. In the case of the Interstate 5 (I-5) Freeway construction along Beacon, First, and Capitol Hills in Seattle (Fig. 1), deep-seated slope failures that occurred shortly after excavating into the hillside were thought to be independent of rainwater or groundwater conditions and were attributed to the release of lateral stress alone (Palladino and Peck 1972; Johnson 1989; Squier and Klasell 1989).

Pressuremeter Device and Testing Procedures

The instrument used in this study was a Cambridge-type (Hughes 1973) prebored pressuremeter (Fig 5). Testing within the very stiff to hard Qpgl was accomplished within prebored 90-cm-long test pockets drilled using a tricone bit with a diameter slightly smaller than that of the pressuremeter. During drilling the smaller bit makes a hole size close to the pressuremeter diameter. Once seated in the test pocket, nitrogen gas is released into the bladder. The applied gas pressure, p, and membrane displacements are measured electronically using a pressure cell and three strain gauges (spaced 120° apart) located within the membrane. Radial membrane displacements, Δr,

J. Geotech. Geoenviron. Eng. 2014.140.

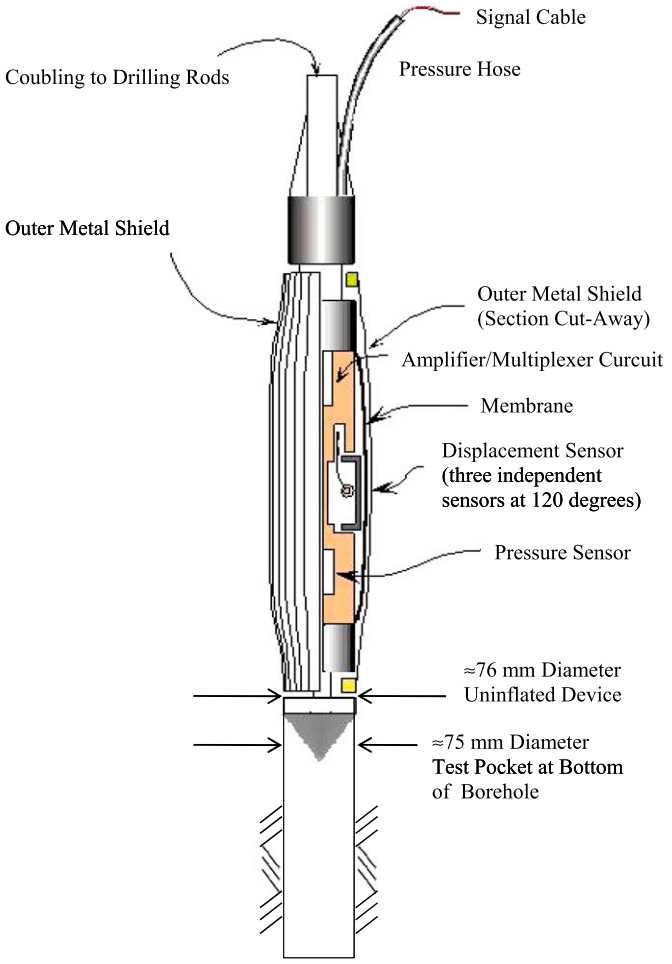

Fig. 5. Details of the high-pressure, prebored pressuremeter device

from the three arms are averaged together and converted to a cavity strain, ε_R ($\equiv \Delta r/r_0$, where r_0 = the initial or reference radius of the pressuremeter membrane). These measurements are transmitted electrically to the ground surface and displayed on a laptop computer. Typically, between 100 and 800 data points (readings once every 5 s) are obtained per test. Each PMT consisted of a loading (expansion) phase, multiple unload-reload loops conducted during the loading phase, an unloading (contraction) phase, and creep tests conducted during the unloading phase.

In situ Lateral Stress Estimation Techniques

Several methods were implemented to estimate lateral stress conditions in the soils encountered along the tunnel alignment. Three pressuremeter methods, including initial curve inspection methods, constitutive modeling (fitting a constitutive model to the field test data), and in situ balance pressure creep testing were performed for this study. These results were compared to laboratory test-based methods using K_0-OCR and K relationships.

Initial Curve Inspection Methods

This type of PMT data reduction analysis involves inspection of the initial portion of the p-ε_R curve to estimate the beginning (corresponding to the in situ total horizontal stress, σ_{h0}) and end (corresponding to the yield point = $\sigma_{h0} + S_{U,\mathrm{LOAD}}$) of the initial elastic portion of the curve. The Marsland and Randolph (1977) method is an example of this type of analysis. Other analyses include correlating the first inflection point in the p-ε_R curve to σ_{h0} (Briaud 1992) and simply using pressure at the first sign of radial strain, or lift-off (Powell 1990), as an estimate of σ_{h0}.

The main advantage of using the initial portion of the PMT p-ε_R curve to estimate σ_{h0} is that, for PMTs with minimal disturbance, σ_{h0} can be observed directly from the data. That said, the main pitfall of this method is that soil disturbance can affect greatly the initial portion of the p-ε_R curve. In the case where the testing pocket is too large or if the surrounding soil is loosened during test pocket creation, the estimated σ_{h0} would likely be too low (if discernible at all). In the case where the pressuremeter is pushed in with a significant amount of force, the surrounding soil may be compacted, which could introduce additional in situ horizontal stresses against the membrane, causing the observed initial stiffness and, therefore, apparent σ_{h0} to be higher than the in situ value.

The Marsland and Randolph (1977) method was attempted on the SR-99 PMT curves but the resulting σ_{h0} values were wildly variable and, thus, were considered to be unreliable. Due to initial disturbance, the lift-off method was not feasible in the SR-99 prebored PMTs in Qpgl.

Constitutive Modeling Approach

The constitutive modeling approach (also referred to as curve fitting or image matching) involves overlaying a simple constitutive soil model over the raw pressuremeter response data (p-ε_R curve). In the current study, the behavior of cohesive material (clays and clayey silts) was approximated using the Gibson and Anderson (1961) clay model. This approach assumes a simple linear-elastic, perfectly-plastic constitutive model for the case of cylindrical cavity expansion. In other words, the model assumes the shear modulus is constant with cavity strain and the undrained shear strength remains constant after plastic yielding has occurred.

The constitutive modeling approach used in this study was described by Jefferies (1988). A detailed description of this approach is not reproduced in this paper. In summary, the Gibson and Anderson (1961) clay constitutive model assumes the p-ε_R curve can be defined by three variables: σ_{h0}, G, and S_U. Jefferies expanded on this model by incorporating the unloading strength, $S_{U,\mathrm{UNLOAD}}$, that can be observed during the unloading stage of the PMT. Figs. 6 and 7 present typical pressuremeter raw data curves and superimposed constitutive model curves.

In modeling the Qpgl behavior, the soil shear modulus, G, was taken to be equal to G_{UR} derived from the unload-reload loops within the raw p-ε_R curve. As indicated in Figs. 6 and 7, G_{UR} values from the various unload-reload loops in the Qpgl were relatively consistent within each test. Owing to disturbance observed in the initial portions of most of the tests (Fig. 7), shear moduli derived from the initial elastic loading stage were considered to be unreliable.

The undrained shear strength for the loading stage, $S_{U,\mathrm{LOAD}}$, was determined in the modeling process following the procedure described by Jefferies (1988). The well-known relationship between S_U and the maximum slope of the postyield portions of the p-ε_R curves plotted in log scale (Gibson and Anderson 1961) and relationships between S_U and the test limit pressure (Gibson and Anderson 1961; Ladanyi 1963; Marsland and Randolph 1977) were used as independent checks.

G and S_U determine the shape of the model p-ε_R curve. Changes in σ_{h0} simply translate the model p-ε_R curve up or down along the p axis. Therefore, once G and S_U are set, σ_{h0} can be adjusted by eye to produce a good match to the raw data curve.

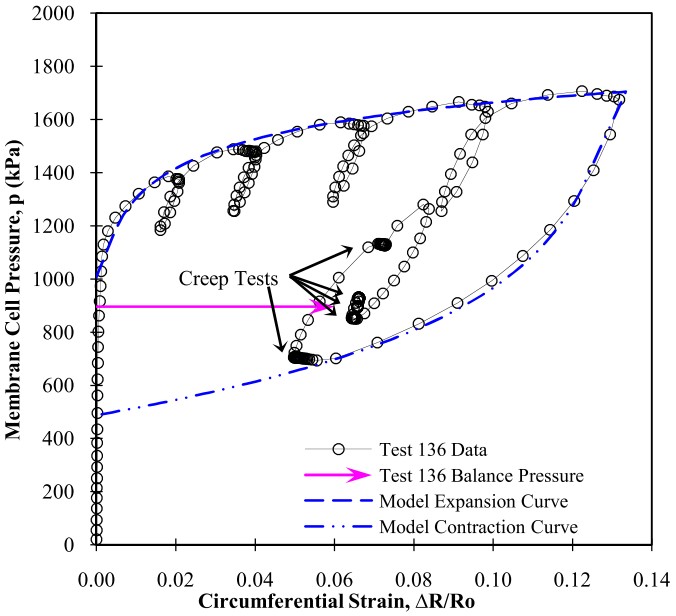

Fig. 6. Raw data, constitutive model curves, and balance pressure point from test 136 from boring TB-321

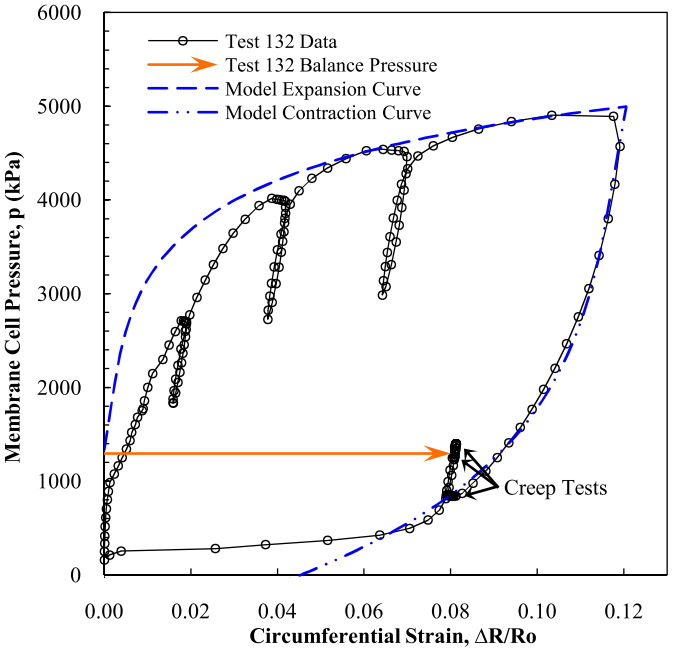

Fig. 7. Raw data, constitutive model curves, and balance pressure point from test 132 from boring TB-320

The limit pressures from PMTs in highly deformed zones of Qpgl were not, as might be expected, lower than tests in relatively intact zones (Table 3). In fact, as in the case of Test 132 (Fig. 7), many of the limit pressures from tests in highly deformed clay were higher than those from tests in relatively intact clay (e.g., Test 136 shown in Fig. 6). Tests 132 and 136 were performed about 30 m apart and at roughly the same elevation but Test 132 indicated a significantly higher limit pressure (Fig. 8). It is also worth noting that the clay at Test 132 had a higher plasticity index than at Test 136 because higher plasticity typically correlates to higher strength (and, therefore, limit

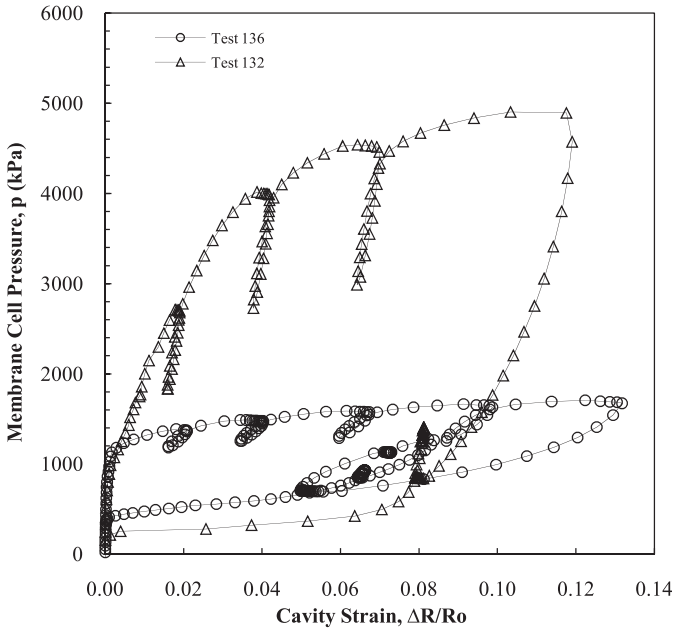

Fig. 8. Raw data from tests 132 and 136 from borings TB-320 and TB-321, respectively

pressure). Both tests exhibited high-quality postyield data and, therefore, are considered good quality tests; the difference in strength evident in Fig. 8 may be due to localized lateral preloading (i.e., bulldozing) during glacial advance.

In situ Balance Pressure Creep Testing

The BPC testing technique was used by Hughes in 1995 (Hughes Insitu Engineering, "Results of Pressuremeter Testing at the LNG Site La Brea, Trinidad," unpublished report) for the investigation of a liquefied natural gas site in a tar formation. Under pressuremeter expansion, the tar behaved as a relatively high-strength, cohesive-type material. On unloading, the pressure was held constant below the anticipated vertical stress. As the pressure remained constant the membrane crept inwards toward the body of the probe. The movement was surprisingly large, on the order of 3–4%, over about 3min. The pressure was then raised to above the estimated vertical stress and the membrane started to move outward. Hence, there seemed to be the possibility of establishing a balance pressure at which the membrane would not move. Given time constraints, this was not done at the Trinidad site. After preliminary phase PMTs indicated higher than expected lateral stresses within Qpgl deposits for the SR-99 Tunnel project, the BPC technique was implemented in the final ten Qpgl PMTs for comparison purposes.

BPC testing was performed during the unloading stage in Qpgl PMTs in boreholes TB-318, TB-320, and TB-321 (Fig. 1). The procedure consists of holding the membrane pressure constant at some point on the unloading curve, and observing whether the membrane moves inward or outward. It is hypothesized that the direction of membrane movement indicates whether the hold pressure is above or below the in situ lateral earth pressure. The number of trial hold pressures for each BPC is summarized in Table 3. Each pressure was held for about 2 min.

Fig. 9 presents a BPC test series in which five hold pressures were performed (test performed during PMT No. SR-99–137). As indicated, the fifth hold pressure iteration of 916 kPa resulted in almost

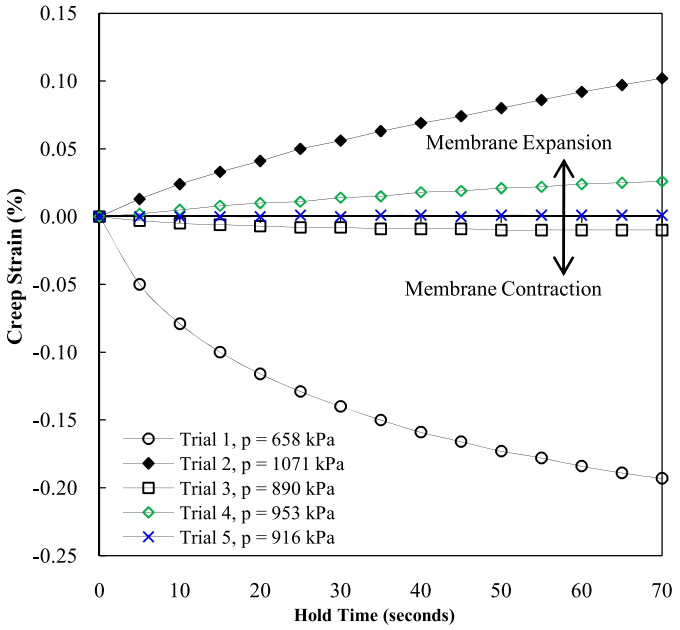

Fig. 9. BPC test results from test SR-99–137

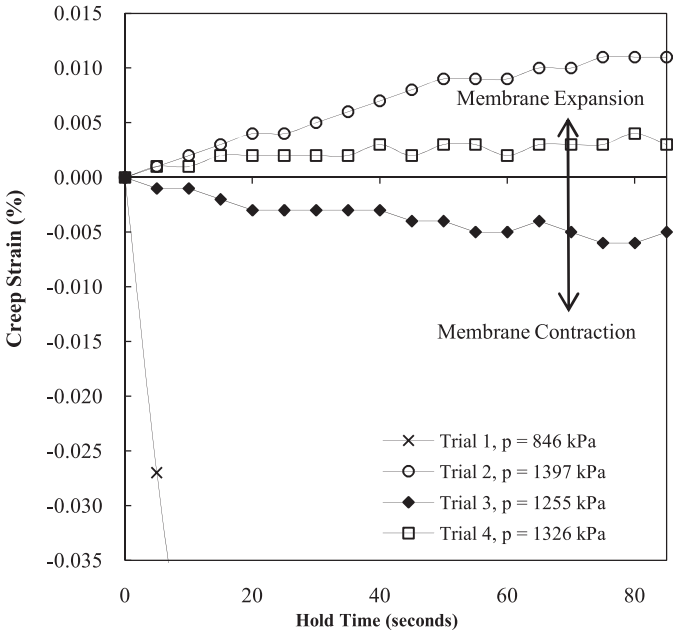

Fig. 11. BPC test results from test SR-99–132

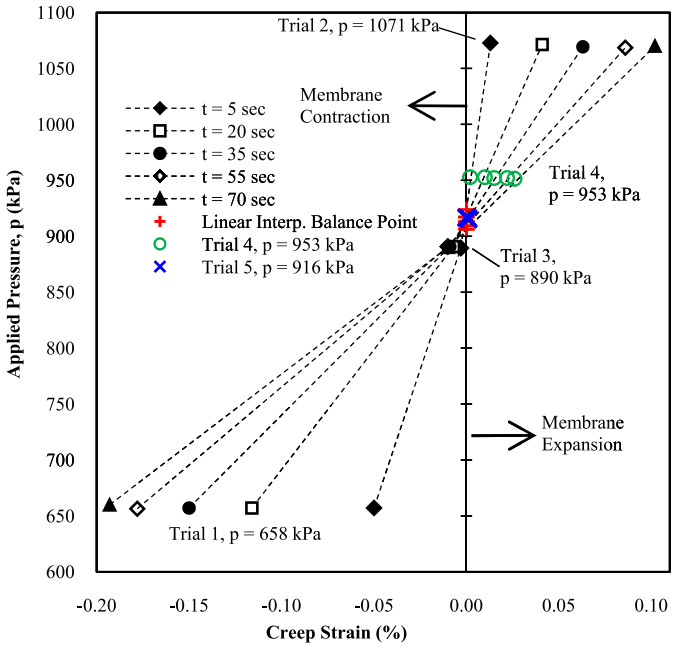

Fig. 10. Applied pressure versus creep strain for various hold times (data from test SR-99–137)

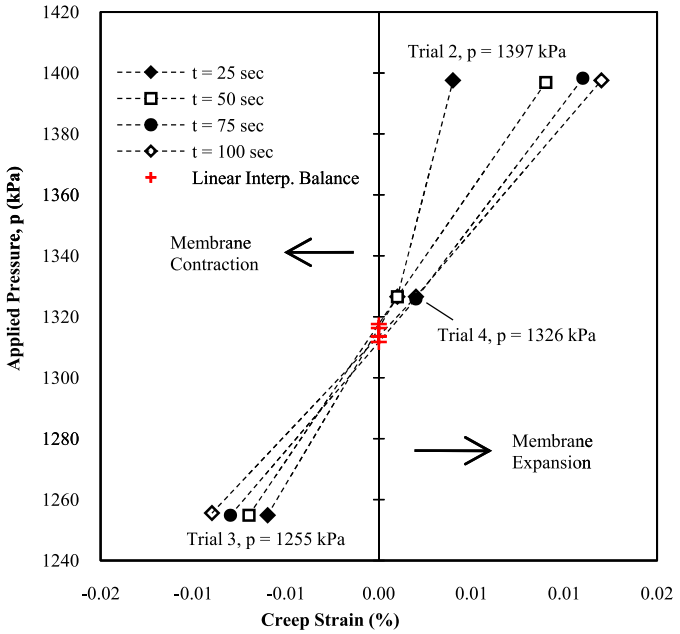

Fig. 12. Applied pressure versus creep strain for various hold times (data from test SR-99–132)

no creep movement and, therefore, was taken as the balance pressure for the Qpgl deposit at the test depth.

It was recognized that the rate of creep strain was proportional to the magnitude of the difference between the balance pressure and the creep test hold pressure. Using this concept, creep strains at various hold times were extracted from each creep test trial data set and plotted versus hold pressure (Fig. 10). The balance pressure point was estimated by interpolating the pressure where the curves intersect the zero creep-strain axis. The test data indicated the hold time curves were roughly linear, but had different slopes on either side of the zero creep-strain axis. To check the validity of this technique, the interpolation curves for PMT No. SR-99–137 were produced using the first three of five creep test trials and plotted together with the final two trials in Fig. 10. As indicated, the interpolation curves and fourth and fifth trial hold pressure points show exceptional agreement.

Creep strain versus hold time and creep strain versus hold pressure for Test SR-99–132 are presented in Figs. 11 and 12, respectively. This test exhibited a higher limit pressure, lower creep strains, and much greater initial disturbance during the expansion phase than Test SR-99–137,and yet still displayed a well-defined balance point using the BPC method.

K_0-OCR and K_0-PI Relationships

Relationships between the coefficient of lateral earth pressure at rest, $K_0 = \sigma'_{h0}/\sigma'_{v0}$, and the overconsolidation ratio, OCR $= \sigma'_{vY}/\sigma'_{v0}$ (where σ'_{vY} = the maximum past vertical effective preconsolidation stress, indicated as Point D in Fig. 4), as well as K_0 and plasticity index (PI) have been observed by many researchers. Two of the most well-established relationships are those of Brooker and Ireland (1965) and Mayne and Kulhawy (1982). Brooker and Ireland related PI and OCR to K_0 and presented the relationship in charts. Mayne and Kulhawy and (1982) developed the following relationship:

$$K_0 = K_{0NC}(\text{OCR})^{\alpha} \tag{1}$$

where K_{0NC} = the value of K_0 during one-dimensional virgin compression (OCR = 1), typically taken as $1 - \sin\phi'$, $\alpha = \sin\phi'$, and ϕ' = the effective stress internal friction angle. Kulhawy and Mayne (1990) recommended using a ϕ' that corresponds to peak failure in conventional triaxial compression (ϕ'_{TC}). Eq. (1) is applicable to a simple unloading stress path (i.e., axisymmetric, one-dimensional loading and unloading).

A total of eight oedometer tests were performed on Qpgl specimens retrieved from the SR-99 tunnel borings. To supplement this limited number of test results, consolidation test results were retrieved from several previous geotechnical studies in the Seattle area. These projects include the following: (1) Beacon Hill Tunnel (Shannon and Wilson, "Geotechnical Data Report, Sound Transit, Central Link Link Light Rail, Seattle, Washington," unpublished report); (2) SR-520 Floating Bridge Replacement and HOV Program (Shannon and Wilson, "Geotechnical Data Report, SR-520 Bridge Replacement and HOV Program, Seattle, Washington," unpublished report); (3) the West Seattle Bridge (Shannon and Wilson, "Geotechnical Engineering Studies, West Seattle Bridge Replacement, Seattle, Washington," unpublished report); (4) I-90 Mercer Island (Converse Consultants, "Report on Geotechnical Investigation, Proposed I-90 East Limits of Mercer Island Tunnel to South Bellevue Interchange," unpublished report); (5) Downtown Transit Tunnel (Shannon and Wilson, "Geotechnical Report, Downtown Seattle Transit Project, Seattle, Washington," unpublished report); (6) the Mount Baker Ridge Tunnel (Shannon and Wilson, "Subsurface Investigations, Proposed Mt. Baker Ridge Tunnel, Seattle, Washington," unpublished report); and (7) Columbia Center (Shannon and Wilson, "Phase 2 Geotechnical Studies, Temporary Shoring System, Columbia Center, Seattle, Washington," unpublished report). A total of 59 consolidation tests performed on specimens of both Qpgl and Qvgl were evaluated for the current study.

While evaluating the effective vertical yield stresses, σ'_{vY}, of these tests, two general observations were made. First, the $e - \log \sigma'_{vc}$ curves, where e = the void ratio and σ'_{vc} = the vertical effective consolidation stress applied in the oedometer, from consolidation tests in Seattle clay exhibit soft or rounded responses at low stresses and do not typically display a well-defined yield point. This behavior has been observed by Grozic et al. (2003) in Norwegian Sea and North Sea glaciomarine clays, and Jefferies et al. (1987) in Beaufort Sea clays. These researchers concluded the most reliable method for estimating σ'_{vY} for clays that exhibit this behavior was proposed by Becker et al. (1987). This method, based on a work per unit volume ($W = \int \sigma'_{vc}\, d\varepsilon_v$, where ε_v = the vertical strain) criterion, identifies σ'_{vY} as the point in W-σ'_{vc} space defined by the intersection of a line fitted to the data points below the in situ vertical effective stress, σ'_{v0}, and a line fitted to the data points at high consolidation stresses that exhibit a linear trend. This introduces the second general observation about past oedometer testing in Seattle clay. Of the 59 consolidation tests evaluated, 27 were either not loaded beyond σ'_{vY}, or were not loaded far enough beyond σ'_{vY} to exhibit a linear trend in W-σ'_{vc} space at high vertical stresses. Determination of reliable σ'_{vY} values for such tests was not feasible using any method owing to the lack of clear virgin compression behavior.

Derived OCR values included in Fig. 13 represent the 32 tests that indicated unambiguous postyield linear W-σ'_{vc} behavior. Based on the consolidation test data, the upper and lower bounds of σ'_{vY} for Seattle clay (the abscissa of Point D of Fig. 4) can be approximated using the following relationship:

$$\sigma'_{v0} + 1.2\,\text{MPa} < \sigma'_{vY} < \sigma'_{v0} + 3.9\,\text{MPa} \tag{2}$$

OCR curves defined by these bounds are plotted in Fig. 13 by assuming the average σ'_{v0} profile from borings TB-318, TB-320, and TB-321. Although it is difficult to determine with certainty what process or combination of processes (e.g., glacial ice loading, complex changes in subglacial porewater pressures, or deposition and erosion of the GLF) caused the maximum past vertical effective stresses in the Seattle clay, these stresses were recorded into the stress memory of the clay and can be observed in the form of σ'_{vY} in oedometer tests. In other words, the specific details of the conceptual stress history shown in Fig. 4, such as when the maximum stresses occurred (whether during the latest Vashon glaciation as indicated in Fig. 4 or perhaps during an earlier glaciation) and whether it was caused entirely from the net ice load or entirely from the GLF or some combination, the *magnitude* of the maximum vertical stress most likely falls within the range described in Eq. (2).

The upper and lower bound OCR profiles from Eq. (2) were input into Eq. (1) to estimate simply unloaded K_0 depth profiles in Fig. 14. A peak ϕ'_{TC} value of 29° (Table 2) was used to estimate K_{0NC} and the unloading parameter α. K_0 ranges using the Brooker and Ireland (1965) chart and data from Table 3 and Eq. (2) are also plotted in Fig. 14.

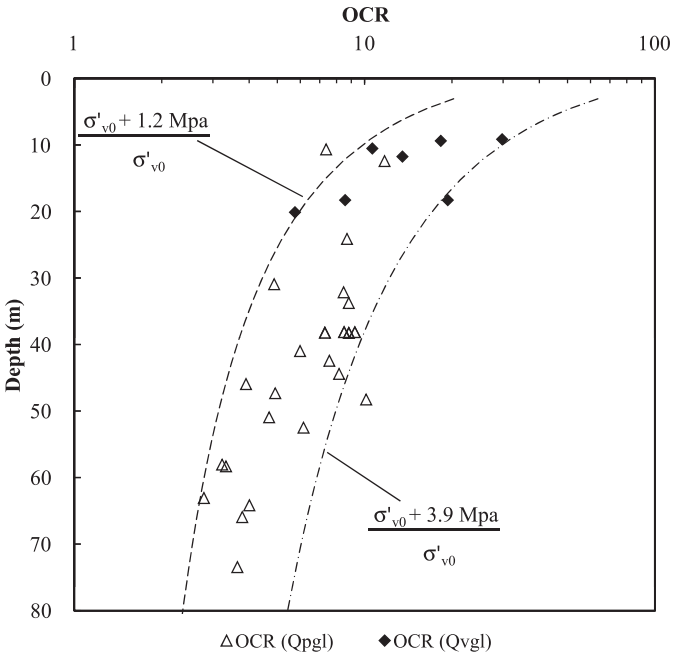

Fig. 13. OCR and maximum oedometer test $\sigma'_{vc}/\sigma'_{v0}$ ratios with depth

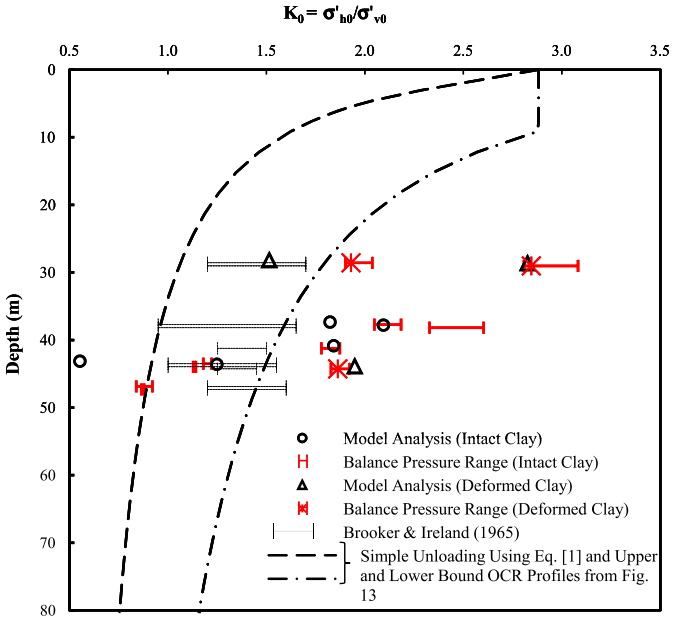

Fig. 14. K_0 with depth from Eq. (1) using $\phi'_{TC} = 29°$ and average subsurface conditions from borings TB-318, TB-320, and TB-321 (dashed line) and from pressuremeter BPC testing and corresponding constitutive model analyses

Discussion of Results

K_0 estimates from the 10 pressuremeter balance creep tests and the constitutive model analyses from the same PMTs are presented in Fig. 14 and Table 3. Most of the K_0 values measured from BPC testing and interpreted from constitutive model fitting were remarkably similar given the methods are so different. However, in tests that displayed significant initial disturbance during initial expansion, the best-fit constitutive model K_0 values tended to be lower than those measured using the BPC test technique. BPC tests conducted in zones of deformed clay are indicated in Fig. 14 and Table 3. The in situ K_0 ranges in the deformed clay seem to be higher than those in the intact clay, but both data sets have a significant overlap. One might expect the deformed clay to have larger K_0 values. However, because the deformed zones are discontinuous in the horizontal direction, the authors speculate the lateral stresses in these zones may have distributed into adjacent, more intact zones since the time of shearing.

As indicated in Fig. 14, many of the pressuremeter-derived K_0 values are significantly higher than what would be expected following simple rebound using either the Mayne and Kulhawy (1982) or Brooker and Ireland (1965) methods. The authors do not consider this to be evidence that challenges these relationships, but rather a real-world example of the ability of clay to retain three-dimensional stress memory. Mesri and Hayat (1993) have shown the horizontal effective stresses, σ'_h, of clay specimens subjected to drained, laterally constrained compression (i.e., oedometer stress path), followed by passive shearing (increasing σ'_h, under constant σ'_v), followed by a reimposition of laterally constrained boundary conditions do not decrease back to a K_{0NC} condition after the excess porewater pressures have dissipated. Instead, they found that roughly 40% of the applied horizontal stresses remained in the specimens after the porewater pressure had dissipated. Further, they proposed that, following passive shearing, K_0 during one-dimensional vertical unloading be estimated by replacing the coefficient K_{0NC} in Eq. (1) with a lateral stress coefficient estimated using the residual or locked-in horizontal stress state after passive shearing (hereafter referred to as K_{0P}).

Although the level of horizontal stress increase because of the advancing (pre-Vashon) ice lobe and formation of the overlying glacial till (Qpgt) is not known, the level of deformation exhibited in many Qpgl samples deformed zones suggests the horizontal stresses were likely high enough to cause localized passive failure (ordinate of Point B in Fig. 4). In other words, K_{0P} may have been on the order of $0.4K_P$ after glacial shearing. Using Eq. (1), this value would result in a current in situ K_0 that is significantly higher than the range estimated in this study. This apparent discrepancy may be because the glacial bulldozing and formation of the overlying Qpgt (during the glaciation that generated the Qpgl deposit in question), which would have caused the highest passive shear stresses in the Qpgl, occurred prior to the GLF deposition and Vashon glaciation. Gudehus et al. (1977) and Topolnicki et al. (1990) showed that, after a change in strain path direction (e.g., from horizontal passive-type straining to laterally constrained vertical loading and rebound), the reorientation of soil particles tends to cause the stress path direction to move asymptotically toward the new strain path direction, which causes the soil to gradually lose its memory of the initial deviatoric stress/strain history.

Summary and Conclusions

A novel technique for estimation of in situ lateral stresses, BPC testing, was performed in 10 PMTs during the geotechnical exploration program for the SR-99 Bored Tunnel project.

The BPC technique was experimental during the SR-99 Bore Tunnel project exploration program and continues to be under development. Improved testing procedures for the BPC technique that attempt to control for possible loading rate and duration effects have been implemented in subsequent projects. Pore pressures develop during undrained PMT loading and also may have some influence on the creep behavior. However, because the pressuremeter membrane is impermeable, these pressures would need to dissipate into the formation. Further, the creep tests are held only for approximately 2 min. The authors anticipate that cavity creep movement is driven by an unbalanced pressure field and not dissipation of porewater. Future experimental studies with pore pressure measurements in a laboratory-controlled environment would be greatly beneficial to help better understand the relationship between cavity expansion creep movement and in situ lateral confining stress.

Despite these uncertain aspects of BPC testing, the in situ lateral stresses derived from the technique were found to be consistent with those derived using constitutive model curve fitting (image matching). However, the stresses were significantly higher than estimated by well-known unloading K_0-OCR and K_0-PI-OCR relationships. In some cases, the OCR and PI relationships underpredict the in situ lateral stress by a factor greater than 2. Based on zones of intense deformation frequently observed in Qpgl, it is likely this clay underwent significant lateral shearing and not the simple, laterally constrained loading and rebound these relationships assume.

High in situ lateral earth pressures have been measured in Seattle clay in the past and have been identified as the primary cause for instability of cut slopes and shored excavations during the I-5/Seattle Freeway construction in the 1960s. Landslides in Seattle clay typically are attributed to rainwater infiltration. However, as shown by Duncan and Dunlop (1969) via finite-element modeling, if the in situ K_0 is doubled in the model, then the estimated maximum shear stress within the toe of the cut slope increased by a factor of two. In other words, the *available* shearing resistance would be considerably lower than that measured by conventional triaxial

testing (isotropic consolidation). Given that very stiff clays such as Qpgl and Qvgl exhibit initially negative (dilative) induced porewater pressures, the initial (undrained) shear strength is typically very high, which usually results in a temporarily stable cut condition. However, once the induced negative porewater pressures dissipate (after days, weeks, months, or years, depending on drainage conditions), the drained shear strength along a potential slip surface may be lower than the applied shear stress. Rainwater or groundwater from sand seams within the clay may infiltrate into fissures/fractures, which may open during unloading. This could break the capillary porewater pressures and expedite failure. However, attributing such failures to infiltrating groundwater alone without consideration of a high K_0 overlooks a critical potential long-term failure mode.

Acknowledgments

The author thank the WSDOT for permission to publish this paper. Thanks also to Red Robinson, Bill Laprade, and Stan Boyle with Shannon and Wilson, Inc. and Dr. Fred Kulhawy with Cornell University for their helpful criticism and advice. Pressuremeter testing was conducted by In Situ Engineering of Snohomish, Washington.

Notation

The following symbols are used in this paper:

G = shear modulus;
G_{UR}. = shear modulus in pressuremeter unload-reload loop;
K_0 = coefficient of lateral earth pressure at rest ($K_0 = \sigma'_{h0}/\sigma'_{v0}$)
K_{0NC} = value of K_0 during one-dimensional virgin compression;
K_P = coefficient lateral earth pressure at the passive state;
OCR = overconsolidation ratio ($OCR = \sigma'_{vY}/\sigma'_{v0}$)
p = cavity pressure;
Q = subglacial meltwater discharge rate;
r_0 = initial or reference radius of the pressuremeter membrane;
$S_{U,LOAD}$ = undrained strength in pressuremeter expansion;
$S_{U,UNLOAD}$ = undrained strength in pressuremeter contraction;
W = work per unit volume in oedometer compression ($W = \int \sigma'_{vc} d\varepsilon_v$);
α = rebound exponent in laterally one-dimensional vertical unloading;
β = ratio $S_{U,UNLOAD}/S_{U,LOAD}$;
Δr = pressuremeter membrane radial displacement;
ε_R = cavity strain ($\varepsilon_R = \Delta r/r_0$)
ε_v = vertical strain in oedometer compression;
σ_{h0} = in situ lateral total stress;
σ'_{h0} = in situ lateral effective stress;
σ'_h = lateral effective stress;
σ'_v = vertical effective stress;
σ'_{vc} = vertical effective consolidation stress applied in oedometer compression;
σ'_{vY} = effective vertical yield stress (also known as the *preconsolidation pressure*)
σ'_{v0} = in situ vertical effective stress;
ϕ' = effective stress internal friction angle; and
ϕ'_{TC} = effective stress internal friction angle in triaxial compression.

References

Andrews, G. H., Squier, L. R., and Klasell, J. A. (1966). "Cylinder pile retaining walls." *Structural Engineering Conf.*, ASCE, Reston, VA.
Becker, D. E., Crooks, J. H. A., Been, K., and Jefferies, M. G. (1987). "Work as a criterion for determining in situ and yield stresses in clays." *Can. Geotech. J.*, 24(4), 549–564.
Booth, D. B. (1991). "Glacier physics of the Puget lobe, southwest Cordilleran ice sheet." *Géographie Physique et Quaternaire*, 45(3), 301–315 (in French).
Booth, D. B. (1994). "Glaciofluvial infilling and scour of the Puget Lowland, Washington, during ice-sheet glaciation." *Geology*, 22(8), 695–698.
Booth, D. B., and Hallet, B. (1993). "Channel networks carved by subglacial water: Observations and reconstruction in the eastern Puget Lowland of Washington." *Geol. Soc. Am. Bull.*, 105(5), 671–683.
Briaud, J. L. (1992). *The pressuremeter*, Balkema, Rotterdam, Netherlands.
Brooker, E. W., and Ireland, H. O. (1965). "Earth pressures at rest related to stress history." *Can. Geotech. J.*, 2(1), 1–15.
Duncan, J. M., and Dunlop, P. (1969). "Slopes in stiff-fissured clays and shales." *J. Soil Mech. Found. Div.*, 95(2), 467–492.
Gibson, R. E., and Anderson, W. F. (1961). "*In situ* measurement of soil properties with the pressuremeter." *Civ. Eng. Public Works Rev.*, 56(658), 615–618.
Grozic, J. L. H., Lunne, T., and Pande, S. (2003). "An oedometer test study on the preconsolidation stress of glaciomarine clays." *Can. Geotech. J.*, 40(5), 857–872.
Gudehus, G., Goldscheider, M., and Winter, H. (1977). "Mechanical properties of sand and clay and numerical integration methods: some sources of errors and bounds or accuracy." Chapter 3, *Finite elements in geomechanics*, G. Gudehus, ed., Wiley, London, 121–150.
Hughes, J. M. O. (1973). "An instrument for *in situ* measurement in soft clays." Ph.D. thesis, Univ. of Cambridge, Cambridge, U.K..
Jefferies, M. G. (1988). "Determination of horizontal in situ stress in clay with self-bored pressuremeter." *Can. Geotech. J.*, 25(3), 559–573.
Jefferies, M. G., Crooks, J. H. A., Becker, D. E., and Hill, P. R. (1987). "Independence of geostatic stress from overconsolidation in some Beaufort Sea clays." *Can. Geotech. J.*, 24(3), 342–356.
Johnson, K. A. (1989). "Foundations Seattle Freeway Construction, Interstate 5: 1960–1966." *Engineering geology in Washington*, R. W. Galster, ed., Vol. II, Washington State Dept. of Natural Resources, Olympia, WA, 773–784.
Kulhawy, F. H., and Mayne, P. W. (1990). "Manual on estimating soil properties for foundation design." *Rep. No. EL-6800*, Electric Power Research Institute (EPRI), Palo Alto, CA.
Ladanyi, B. (1963). "Expansion of a cavity in a saturated clay medium." *J. Soil Mech. and Found. Div.*, 89(SM4), 127–161.
Laprade, William T. (1982). "Geologic implications of pre-consolidated pressure values, Lawton clay, Seattle, Washington." *Proc., 19th Engineering Geology and Soils Engineering Symp.*, Transportation Dept., Boise, ID, 303–321.
Marsland, A., and Randolph, M. F. (1977). "Comparisons of the results from pressuremeter tests and large in situ plate tests in London clay." *Géotechnique*, 27(2), 217–243.
Mayne, P. W., and Kulhawy, F. H. (1982). "K_0-OCR relationships in soil." *J. Geotech. Engrg. Div.*, 108(6), 851–872.
Mesri, G., and Hayat, T. M. (1993). "The coefficient of earth pressure at rest." *Can. Geotech. J.*, 30(4), 647–666.
Miller, J. A. (1989). "Landslide stabilization in an urban setting, Fauntleroy district, Seattle, Washington." *Engineering geology in Washington*, R. W. Galster, ed., Vol. II, Washington State Dept. of Natural Resources, Olympia, WA, 681–690.
Palladino, D. J., and Peck, R. B. (1972). "Slope failures in an overconsolidated Clay, Seattle, Washington." *Géotechnique*, 22(4), 563–595.

Powell, J. J. M. (1990). "A comparison of four different pressuremeters and their methods of interpretation in a stiff, heavily overconsolidated clay." *3rd. Int. Symposium on Pressuremeters*, Thomas Telford, London, 287–298.

Rowe, P. W. (1972). "The relevance of soil fabric to site investigation practice." *Géotechnique*, 22(2), 195–300.

Sherif, M. A., and Strazer, R. J. (1973). "Soil parameters for design of Mt. Baker Ridge tunnel in Seattle." *J. Soil Mech. Found. Div.*, 99(1), 111–122.

Sherif, M. A., and Wu, M. J. (1971). "Summary and practical implications of the University of Washington soil and engineering research (1965-1970)", *Univ., of Washington Soil Engineering Final Report*, Univ. of Washington, Seattle.

Skempton, A. W., Schuster, R. L., and Petley, D. J. (1969). "Joints and fissures in the London clay at Wraysbury and Edgware." *Géotechnique*, 19(2), 205–217.

Squier, L. R., and Klasell, J. A. (1989). "Cylinder pile walls along interstate highway 5, Seattle." *Engineering geology in Washington*, R. W. Galster, ed., Vol. II, Washington State Dept. of Natural Resources, Olympia, WA, 785–796.

Strazer, R. J., Bestwick, L. K., and Wilson, S. D. (1972). "Design considerations for deep retained excavations in over-consolidated Seattle clays." *Workshop on Expansive Clays and Shales in Highway Design and Construction*, Federal Highway Administration, Denver.

Thorson, R. M. (1989). "Glacio-isostatic response of the Puget Sound area, Washington." *Geol. Soc. Am. Bull.*, 101(9), 1163–1174.

Topolnicki, M., Gudehus, G., and Mazurkiewicz, B. K. (1990). "Observed stress-strain behavior of remolded saturated clay under plane strain conditions." *Géotechnique*, 40(2), 155–187.

Troost, K. G., and Booth, D. B. (2008). "Geology of Seattle and the Seattle area, Washington." *Geological Society of America reviews in engineering geology XX: Landslides and engineering geology of the Seattle, Washington, area.* R. L. Baum, J. W. Godt, and L. M. Highland, eds., Geological Society of America Boulder, CO, 1–35.

Washington State DOT (WSDOT). (2012). "Geotechnical design manual." *Manual M46-03.07*, Olympia, WA.